Apoptosis (2019) 24:312–325
https://doi.org/10.1007/s10495-019-01515-1

# Chemotherapeutic paclitaxel and cisplatin differentially induce pyroptosis in A549 lung cancer cells via caspase-3/GSDME activation

**Cheng-cheng Zhang[1] · Chen-guang Li[1] · Yao-feng Wang[1] · Li-hui Xu[2] · Xian-hui He[1] · Qiong-zhen Zeng[1] · Chen-ying Zeng[1] · Feng-yi Mai[1] · Bo Hu[3] · Dong-yun Ouyang[1]**

Published online: 1 February 2019


## Abstract

Gasdermin E (GSDME) has an important role in inducing secondary necrosis/pyroptosis. Upon apoptotic stimulation, it can be cleaved by activated caspase-3 to generate its N-terminal fragment (GSDME-NT), which executes pyroptosis by perforating the plasma membrane. GSDME is expressed in many human lung cancers including A549 cells. Paclitaxel and cisplatin are two representative chemotherapeutic agents for lung cancers, which induce apoptosis via different action mechanisms. However, it remains unclear whether they can induce GSDME-mediated secondary necrosis/pyroptosis in lung A549 cancer cells. Here we showed that both paclitaxel and cisplatin evidently induced apoptosis in A549 cells as revealed by the activation of multiple apoptotic markers. Notably, some of the dying cells displayed characteristic morphology of secondary necrosis/pyroptosis, by blowing large bubbles from the cellular membrane accompanied by caspase-3 activation and GSDME-NT generation. But the ability of cisplatin to induce this phenomenon was much stronger than that of paclitaxel. Consistent with this, cisplatin triggered much higher activation of caspase-3 and generation of GSDME-NT than paclitaxel, suggesting that the levels of secondary necrosis/pyroptosis correlated with the levels of active caspase-3 and GSDME-NT. Supporting this, caspase-3 specific inhibitor (Ac-DEVD-CHO) suppressed cisplatin-induced GSDME-NT generation and concurrently reduced the secondary necrosis/pyroptosis. Besides, GSDME knockdown significantly inhibited cisplatin- but not paclitaxel-induced secondary necrosis/pyroptosis. These results indicated that cisplatin induced higher levels of secondary necrosis/pyroptosis in A549 cells than paclitaxel, suggesting that cisplatin may provide additional advantages in the treatment of lung cancers with high levels of GSDME expression.

**Keywords** Pyroptosis · Secondary necrosis · Cisplatin · Paclitaxel · GSDME · Caspase-3

## Introduction

Lung cancer is among the most dangerous cancers worldwide. In China, it is one of the major causes of cancer-related death. To date, the death rate of lung cancer is more than 6/1000, accounting for over one-fifth of all tumor deaths in China [1], and the five-year survival rate is less than 20% [2]. The current treatment methods include surgery, chemotherapy and radiotherapy, among which chemotherapy is the main strategy for lung cancer treatment.

Paclitaxel and cisplatin (cis-dichlorodiammineplatinum II) are two first-line chemotherapy drugs for treatment of non-small-cell lung cancer (NSCLC) and a wide range of other malignancies [3, 4]. Mechanically, paclitaxel targets the microtubule, decreasing microtubule dynamics in the mitotic spindle, and thereby resulting in G2/M cell cycle arrest and apoptosis, which is characterized by cellular

Cheng-cheng Zhang, Chen-guang Li and Yao-feng Wang contributed equally to this work.

**Electronic supplementary material** The online version of this article (https://doi.org/10.1007/s10495-019-01515-1) contains supplementary material, which is available to authorized users.

✉ Bo Hu
42089537@qq.com

✉ Dong-yun Ouyang
touyangdy@jnu.edu.cn

[1] Department of Immunobiology, College of Life Science and Technology, Jinan University, Guangzhou, China

[2] Department of Cell Biology, College of Life Science and Technology, Jinan University, Guangzhou, China

[3] Department of Nephrology, The First Affiliated Hospital of Jinan University, Guangzhou, China

shrinkage, membrane blebbing, chromatin condensation and formation of apoptotic bodies [5]. It can also potently induce α-tubulin acetylation; and the acetylated α-tubulin is located with the microtubule organization center (MTOC), which may also change the dynamics of microtubules [6]. Indeed, at high concentrations, paclitaxel suppresses microtubule detachment from the centrosomes [7]. But the anticancer mechanism of cisplatin is different from that of paclitaxel. As the first member of platinum-based anticancer drugs, cisplatin is a DNA-damaging agent that can enter cells to cause DNA cross-linking. After administration, one of the two chloride atoms in cisplatin is slowly displaced by water (aquation), making it easily enter cells and crosslink the DNAs. This leads to DNA damage thus activating the DNA repair machinery [8, 9]. As the DNA repair process is unsuccessful after cisplatin treatment [8, 9], pro-apoptotic pathways are triggered leading to the activation of apoptotic executioner caspases (including caspase-3 and -7) and subsequently apoptosis [10].

Recent studies reveal that, apart from executing apoptosis, chemotherapy drug-activated caspase-3 can also induce secondary necrosis/pyroptosis in both cancer and normal cells that express high levels of gasdermin E (GSDME) [11, 12]. Like gasdermin D (GSDMD), GSDME is another member of gasdermin family, of which the N-terminal domain linked to the C-terminal domain. Active caspase-3 cleaves GSDME in its middle linker to generate the N-terminal fragment of GSDME (GSDME-NT) [11, 12]. GSDME-NT will subsequently translocate to and perforate the membrane thereby disrupting the osmotic barrier of the cell leading to necrosis [11, 12]. Such necrosis is a form of programmed cell death named pyroptosis or secondary necrosis. Morphologically, the cells undergoing pyroptotic cell death display ballooning phenotypes with large bubbles blowing from the plasma membrane, which are different from those cells undergoing apoptosis with a marker of blebbing [11–13].

Previous studies have shown that cisplatin and paclitaxel can activate caspase-3 and -7 thus inducing apoptosis in cancer cells [14]. However, it is unclear whether they could induce secondary necrosis/pyroptosis in GSDME-expressing cancer cells. In this study, we used lung cancer A549 cells, which have been shown to express GSDME protein [11, 15], as a cellular model of NSCLC [16] to explore the forms of cell death after being exposed to cisplatin and paclitaxel. Our data demonstrated that both cisplatin and paclitaxel induced apoptosis and secondary necrosis/pyroptosis in A549 cells, but cisplatin triggered more pronounced secondary necrosis/pyroptosis, and higher levels of caspase-3 activation and GSDME-NT generation than paclitaxel did. These results suggest that paclitaxel and cisplatin induced differential patterns of cell death likely due to distinct activation of caspase-3 and cleavage of GSDME in A549 lung cancer cells.

## Materials and methods

### Reagents

Hoechst 33342, propidium iodide (PI) and dimethyl sulfoxide (DMSO) were purchased from Sigma–Aldrich (St. Louis, MO, USA). Paclitaxel (PTX, #P106868) was acquired from Aladdin (Shanghai, China). Cisplatin (DDP, #S1166) and etoposide (#S1225) were bought from Selleck (Houston, TX, USA). CPT-11 (Irinotecan) (#HY-16562A) and Ac-DEVD-CHO (#HY-P1001) were purchased from MedChem Express (Princeton, NJ, USA). PTX, DDP, etoposide and CPT-11 were dissolved in DMSO at 50 mM, and stored at − 20 °C. Dulbecco's Modified Eagle Medium (DMEM), streptomycin, penicillin, fetal bovine serum (FBS), Lipofectamine RNAiMAX Reagent (#13778075) and Opti-MEM (#31985062) were obtained from Thermo/Fisher/Invitrogen (Carlsbad, CA, USA). The antibodies against caspase-3 (#9665), cleaved caspase-7 (#8438), cleaved caspase-8 (#9496), cleaved caspase-9 (#7237), PARP (#9532), GSDMD (#96458) and horse-radish peroxidase (HRP)-conjugated goat anti-rabbit IgG (#7074) were products of Cell Signaling Technology (Danvers, MA, USA). The antibody against DFNA5/GSDME (#ab215191) was obtained from Abcam (Cambridge, UK). The antibody against actin (#sc-1616-R) was bought from Santa Cruz (Dallas, TX, USA). Fixable Viability Dye eFluor660 (#65-0864) was from eBioscience (San Diego, CA, USA). PE Annexin V apoptosis detection kit I (#559763) was obtained from BD Biosciences Pharmingen (San Diego, CA, USA).

### Cell line culture

The human lung adenocarcinoma epithelial cell line A549 was obtained from the American Type Culture Collection (ATCC; Manassas, VA, USA). The cells were maintained in complete DMEM medium (containing 10% FBS, 100 IU/ml penicillin, 100 µg/ml streptomycin and 2 mM L-glutamine) and cultured at 37 °C in a humidified incubator with 5% $CO_2$. The cells were sub-cultured every 2–3 days.

### Cell viability assay

A549 cells in log phase were prepared by seeding them in a 96-well plate at 4000 cells/well and cultured overnight as indicated above. They were treated with indicated concentrations of paclitaxel or cisplatin for 48 h. Then, 10 µl of WST-1 reagent (#11644807001, Roche Diagnostics, Mannheim, Germany) was added to each well, and the plate was further incubated for 1 h at 37 °C. The absorbance was read at 450 nm with a reference at 630 nm using a microplate

reader (Model 680; Bio-Rad, Hercules, CA, USA), and the 50% inhibiting concentrations ($IC_{50}$ values) of these drugs were determined from dose–response curves.

### Lytic cell death assay

Lytic cell death was measured by PI incorporation as described previously [17]. Briefly, cells were seeded in 24-well plates and treated with indicated concentrations of paclitaxel or cisplatin. Cell nuclei were revealed by Hoechst 33342 staining (5 μg/ml, staining for all cells) and PI (2 μg/ml, staining for necrotic cells) for 10 min at room temperature. The cells were observed by live imaging using Zeiss Axio Observer D1 microscope equipped with a Zeiss LD Plan-Neoflar 20 × or 40 × objective lens (Carl Zeiss Micro-Imaging GmbH, Göttingen, Germany). Fluorescence images were captured with a Zeiss AxioCam MR R3 cooled CCD camera controlled with ZEN software (Carl Zeiss).

### Western blot analysis

Preparation of whole cell lysates and western blotting were performed as previously described [18]. In brief, cells were lysed with 2 × sodium dodecyl sulfate-polyacrylamide gel electrophoresis (SDS-PAGE) loading buffer, and the total proteins were separated by SDS-PAGE and then transferred onto a PVDF membrane (#03010040001; Roche Diagnostics GmbH, Mannheim, Germany). The membrane was blocked and incubated with primary antibody overnight, followed by incubation with HRP-conjugated goat anti-rabbit IgG. Bands on the membrane were revealed by a BeyoECL Plus kit (BeyoECL Plus; P0018; Beyotime, Shanghai, China) and recorded on X-ray films (Carestream, Xiamen, China). Images were captured by using FluorChem 8000 Imaging System (Alpha Innotech; San Leandro, CA, USA).

### Small interfering RNA (siRNA)

The siRNA (5′-GGTCCTATTTGATGATGAA-3′) duplexes targeting human *GSDME* (*DFNA5*) and negative control siRNA were designed and synthesized by RiboBio (Guangzhou, China). siRNA transfection was performed using Lipofectamine RNAiMAX Reagent according to the instructions provided by the supplier. The siRNA was added to each well at a final concentration of 100 nM. Cells were cultured in DMEM medium containing 10% FBS for 72 h.

### Flow cytometry analysis

For annexin V and 7-aminoactinomycin D (7-AAD) staining, cells were harvested, washed twice with cold-PBS, and stained with PE Annexin V apoptosis detection kit I according to the manufacturer's instructions. Briefly, the cells were double-stained with annexin V and 7-AAD in binding buffer for 15 min at room temperature. The cells were then analyzed by flow cytometry using Attune NxT acoustic focusing cytometer (ThermoFisher Scientific; Carlsbad, CA, USA). Data were acquired and analyzed with Attune NxT software (Thermo Fisher Scientific).

Fixable viability dye (FVD) eFluor660 was used to irreversibly label dying cells according to the manufacturer's instructions. In brief, cells were washed and re-suspended in cold PBS, then stained with FVD eFluor660 for 30 min at 4 °C. The cells were analyzed by flow cytometry (Attune NxT).

### Mitochondrial membrane potential measurement

The mitochondrial membrane potential was determined by mitochondrial membrane potential assay kit with JC-1 (5, 5′,6, 6′-tetrachloro-1, 1′,3, 3′-Tetraethylbenzimidazolyl-carbocyanine iodide) (Beyotime; Shanghai, China) according to the manufacturer's instructions. In brief, cells were stained with JC-1 working solution for 30 min at 37 °C, washed twice with JC-1 staining buffer, and observed under a fluorescence microscopy (Zeiss Axio Observer D1 microscope). The ratio of JC-1 aggregate/monomer was analyzed by the Image J program (NIH, Bethesda, MD, USA).

### Statistical analysis

All experiments were performed three times independently. Data were presented as mean ± standard deviation (SD). Statistical analysis was performed using GraphPad Prism 5.0 (GraphPad Software Inc., San Diego, CA, USA). One-way analysis of variance (ANOVA) followed by Tukey post hoc test and unpaired Student's t-test was used to analyze the statistical significance among multiple groups and between two groups, respectively. $P$-values < 0. 05 were considered statistically significant.

## Results

### Paclitaxel and cisplatin induced distinct patterns of apoptosis and lytic cell death in A549 cells

To compare the effects of paclitaxel and cisplatin on induction of cell death in lung cancer A549 cells, we first detected the cytotoxicity of these drugs by using WST-1 assay. Paclitaxel did not reach the 50% cell inhibition ($IC_{50}$) of cell viability while the $IC_{50}$ value of cisplatin was about 25 μM after 48 h-treatment, showing different cell death rates at the same concentrations of the two drugs. To further reveal the discrepancy of the cell death induced by these two drugs, we used annexin-V/7-AAD staining together

with flow cytometry to analyze the cells after being treated with these drugs for 24 h. Similar concentrations of these drugs were used and the results showed that both paclitaxel and cisplatin dose-dependently induced apoptosis (annexin-$V^+$/7-$AAD^-$ cells) and necrosis (annexin-$V^+$/7-$AAD^+$ cells) in the cells, respectively (Fig. 1a). At a low concentration (6.7 μM), paclitaxel treatment resulted in higher levels of apoptosis (annexin-$V^+$/7-$AAD^-$ cells) as compared with cisplatin treatment. But at a high concentration (60 μM), they induced comparable apoptosis, and cisplatin induced much higher levels of lytic cell death (annexin-$V^+$/7-$AAD^+$ cells) than paclitaxel did (Fig. 1b, c). These results suggest that paclitaxel and cisplatin induced differential patterns of cell death in A549 cells, which was to be further explored using the same concentrations of paclitaxel and cisplatin (6.7, 20 and 60 μM).

We next used two additional approaches to verify the annexin V/7-AAD staining data of lytic cell death (necrosis): staining the cells with fixable viability dye (FVD) and propidium iodide (PI), both of which can penetrate into the dying cells with the loss of cell membrane integrity. FVD stained cells were analyzed by flow cytometry while PI stained cells were observed by fluorescence microscopy. Consistent with 7-AAD staining, FVD staining assay showed that 60 μM cisplatin treatment for 24 h induced higher levels of lytic cell death than paclitaxel did in A549 cells (Fig. 2a). Similarly, PI staining also showed that the proportions of cisplatin-induced lytic cell death (PI-positive cells) were higher than that of paclitaxel group. Of note, longer treatment (48 h) with cisplatin resulted in more lytic cell death in a dose-dependent manner, whereas paclitaxel induced low levels of lytic cell death without obvious dose-dependent effect (Fig. 2b, c, and Supplementary Fig. 1). Together, these results indicated that cisplatin induced lytic cell death (necrosis) more severely than paclitaxel did in A549 cells.

To further reveal the features of lytic cell death induced by paclitaxel and cisplatin, we observed the morphology of the cells stained with PI by fluorescence microscopy. Upon paclitaxel treatment, the cells got round, and underwent cell shrinkage and blebbing with the cell membrane integrity being retained (PI-negative) (Fig. 2b, white arrow head). After cisplatin treatment, many cells also displayed cell

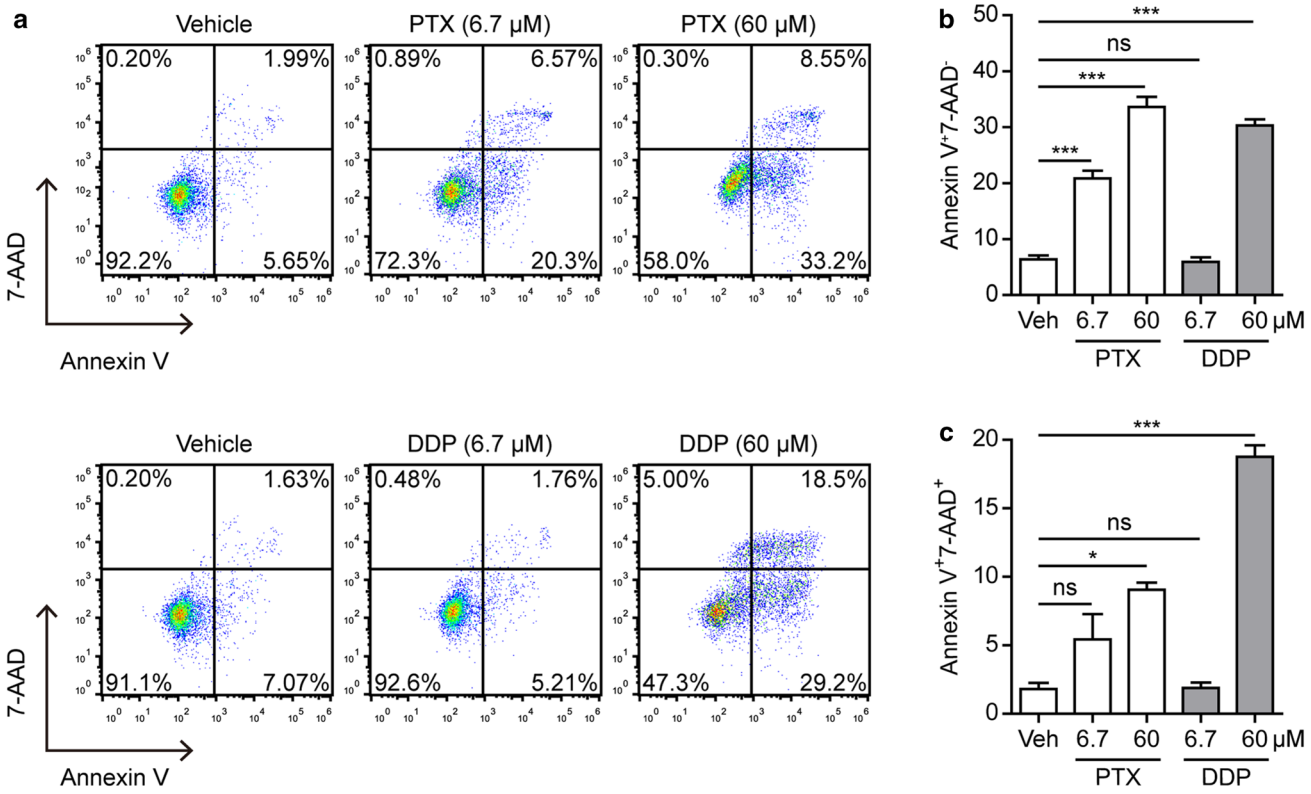


**Fig. 1** Paclitaxel and cisplatin induced apoptosis and lytic cell death in A549 cells. **a**–**c** A549 cells were treated with indicated concentrations of paclitaxel (PTX) and cisplatin (DDP) respectively for 24 h. The cells were stained using the PE-annexin V and 7-aminoactinomycin D (7-AAD) and analyzed by flow cytometry. **a** Representative dot-plots of flow cytometry. Numbers represent the ratios of cells in each quadrant. Annexin-$V^-$/7-$AAD^-$ represented live cells, annexin-$V^+$/7-$AAD^-$ represented apoptotic cells and annexin-$V^+$/7-$AAD^+$ indicated the necrotic or pyroptotic cells. **b, c** Quantitative analysis of the ratios of annexin-V/$7^+AAD^-$ (**b**) and annexin-$V^+$/7-$AAD^+$ (**c**) cells in (**a**). Data are shown as mean ± SD ($n=3$). *$P<0.05$; ***$P<0.001$; *ns* not significant, *Veh* vehicle

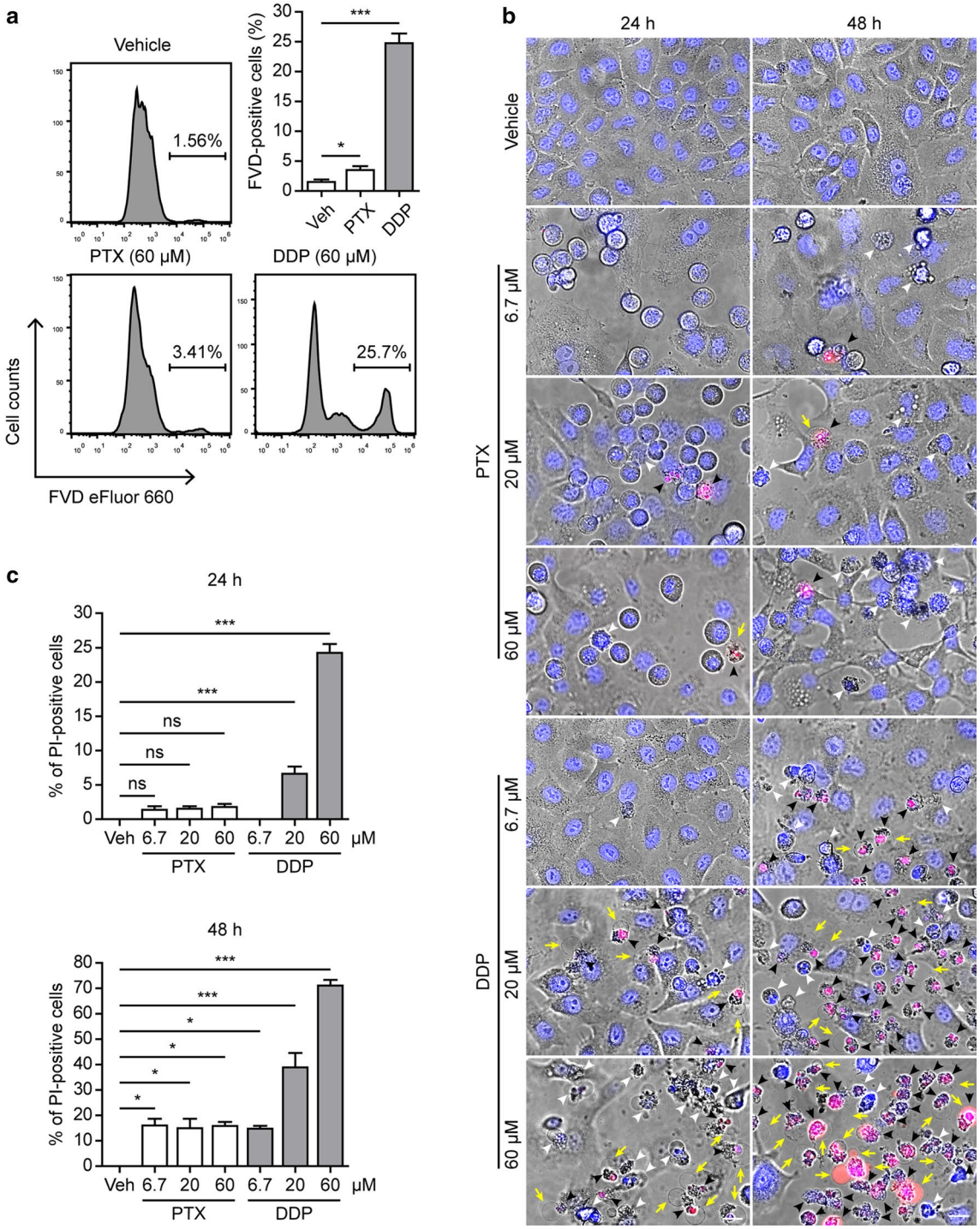


**Fig. 2** Cisplatin induced lytic cell death more potently than paclitaxel in A549 cells. **a** Cells were stimulated with paclitaxel (60 μM) or cisplatin (60 μM) for 24 h, respectively, and then stained with fixable viability dye (FVD) eFluor 660. The cells were analyzed by flow cytometry and representative histograms are shown. Numbers above the markers are dying cells stained by FVD. **b, c** Cells were treated with graded concentrations of paclitaxel and cisplatin for 24 h or 48 h, respectively. The cells were then stained with 2 μg/ml propidium iodide (PI; red, staining dying cells) plus 5 μg/ml Hoechst 33342 (blue, staining all cells) for 10 min, and then observed by fluorescent microscopy (20× or 40× objective lens). **b** One set of representative images of three independent experiments are shown. White arrow heads indicate apoptotic cells; black arrow heads indicate PI-positive (necrotic) cells; yellow arrows indicate lytic (necrotic or pyroptotic) cells with large bubbles blowing from the cellular membrane. Scale bars, 20 μm. **c** PI-positive cells in five random fields (20× objective lens, around 100–150 cells per field) were calculated and statistically analyzed. Data are shown as mean ± SD ($n = 5$). $^{*}P < 0.05$; $^{***}P < 0.001$; *ns* not significant, *DDP* cisplatin; *PTX* paclitaxel; *Veh* vehicle

shrinkage and blebbing but their cell membrane integrity was damaged as evidenced by PI-positive staining (Fig. 2b, black arrow head). Importantly, the PI-positive cells had large bubbles blowing from the plasma membrane (Fig. 2b, yellow arrow), which has been regarded as a typical characteristic of secondary necrosis/pyroptosis different from apoptosis [11]. In contrast, lytic cell death (PI-positive staining) was only observed in a small quantity of paclitaxel-treated cells throughout the treatment period (Fig. 2b, white arrow head). Consistent with previous reports showing that A549 cells are resistant to paclitaxel [19], increased paclitaxel concentrations (up to 240 μM considering its solubility) did not increase the proportion of PI-positive cells or the number of cells with a large bubble within 24 h. But longer treatment (48 h) of paclitaxel increased the number of PI-positive cells, and more typical pyroptotic cells were observed at this time point (Supplementary Fig. 2). These results suggested that both paclitaxel and cisplatin induced secondary necrosis/pyroptosis, but the action of paclitaxel was delayed with much weaker efficacy in inducing secondary necrosis/pyroptosis as compared to that of cisplatin at the same concentrations, highlighting their differential action mechanisms in inducing cell death in cancer cells.

As cisplatin targets the genomic DNA, we further detected whether other DNA drugs also induced secondary necrosis/pyroptosis in A549 cells. As expected, both CPT-11 (an inhibitor of DNA topoisomerase I that causes single-strand DNA breaks) and etoposide (an inhibitor of DNA topoisomerase II that causes double-strand DNA breaks) induced secondary necrosis/pyroptosis, and the latter seemed stronger than the former in inducing such a phenomenon when compared at the same concentrations (Supplementary Figs. 3 and 4). These results showed that A549 cells were sensitive to lytic cell death induced by DNA-damaging drugs (including cisplatin, CPT-11 and etoposide).

## Paclitaxel, but not cisplatin, reduced the mitochondrial membrane potential of A549 cells

As paclitaxel binds microtubules but cisplatin targets genomic DNA, we next investigated whether they induced apoptosis in A549 cells through the intrinsic apoptosis pathway. The mitochondrial membrane potential (ΔΨm) was detected using JC-1 staining. The result showed that paclitaxel significantly decreased the levels of JC-1 aggregates (red) as well as its ratio to JC-1 monomers (green), indicating a reduction of ΔΨm. However, cisplatin did not significantly induce ΔΨm reduction (Fig. 3a, b, and Supplementary Fig. 5). These results suggested that the reduction of ΔΨm might have mediated paclitaxel-induced activation of the intrinsic apoptotic pathway but not be sufficient to explain the effect of cisplatin on inducing the cell death.

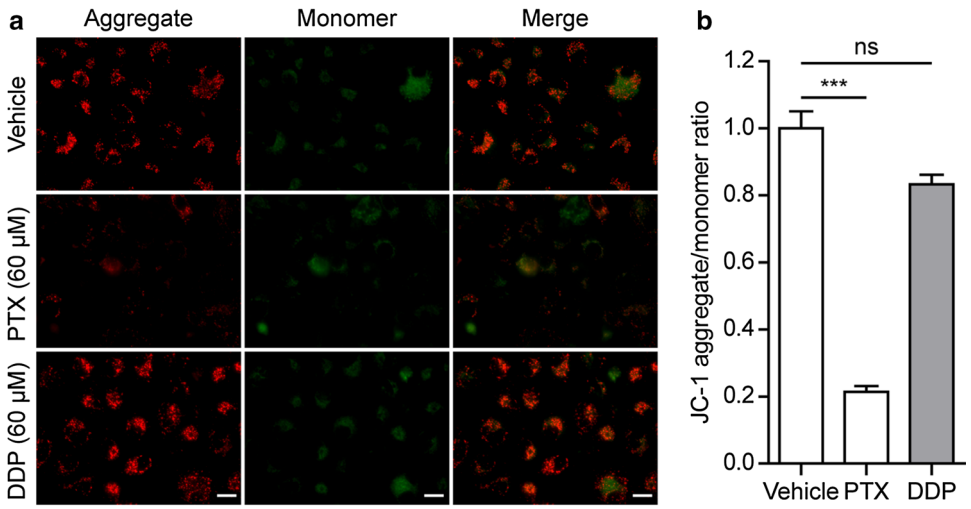


**Fig. 3** Paclitaxel, but not cisplatin, induced reduction of the mitochondrial membrane potential. **a** A549 cells were treated with 60 μM paclitaxel (PTX) or cisplatin (DDP) for 24 h, respectively. Then the mitochondrial membrane potential (ΔΨm) was determined by JC-1. The cells were observed by fluorescence microscopy (20× or 40× objective lens). **a** One representative set of images (40× objective lens) of three independent experiments are shown. The red fluorescence represents the mitochondrial aggregate form of JC-1, indicating high ΔΨm, while the green fluorescence represents the monomeric form of JC-1, indicating the dissipation of ΔΨm. Scale bars, 20 μm. **b** The ratios of JC-1 aggregate/monomer were analyzed by the Image J program. Data are shown as mean ± SD ($n=5$). ***$P<0.001$; *ns* not significant

## Both intrinsic and extrinsic apoptotic pathways had been activated in paclitaxel and cisplatin-treated A549 cells

To investigate the underlying mechanisms by which paclitaxel and cisplatin respectively induced apoptosis and lytic cell death in A549 cells, we analyzed the activation of apoptotic markers by Western blot analysis. The results showed that the apoptotic initiator caspase-8 and -9 were activated (by detecting their cleaved fragments) in paclitaxel- and cisplatin-treated cells in a time-dependent manner (Fig. 4a, b), although their activation levels were more pronounced in cisplatin-treated cells than in paclitaxel-treated ones. Consistent with this, the downstream executioner caspase-3 and -7 were correspondingly activated, accompanied by the cleavage of their substrate poly (ADP-ribose) polymerase (PARP) to produce an 89 kDa fragment (Fig. 4a, b).

We also determined the dose-dependent effects of paclitaxel and cisplatin on apoptosis markers after 24 h treatment. Western blotting revealed that cisplatin dose-dependently induced both apoptotic initiator caspase-8/-9 and executioner caspase-3/-7 activation (Fig. 4c, d). However, paclitaxel showed a much weaker ability in inducing the activation of these caspases, in comparison with the same concentrations of cisplatin (6.7, 20 and 60 μM) (Fig. 4c, d). It only showed a dose-dependent effect in activating these caspases at higher concentrations (60–240 μM) but the effect was still weak as compared with 60 μM cisplatin (Supplementary Fig. 6). Consistent with the weak activation of caspase-3/-7 by paclitaxel, the cleavage of PARP was only weakly detected in paclitaxel-treated cells (Fig. 4, Supplementary Fig. 6). In stark contrast, cisplatin treatment induced pronounced cleavage of PARP as a result of robust caspase-3/-7 activation (Fig. 4c, d). Together, these results indicated that cisplatin induced more pronounced activation of both intrinsic and extrinsic apoptotic pathways than paclitaxel did in A549 cells.

## Activation of caspase-3 was associated with GSDME cleavage and lytic cell death in paclitaxel and cisplatin-treated A549 cells

Recent studies have identified GSDME as a new substrate of caspase-3, which plays a critical role in determining the forms of cell death in response to apoptotic stimulation. Activated caspase-3 cleaves GSDME to generate a fragment named GSDME-NT (37 kDa), which perforates the plasma membrane leading to secondary necrosis/pyroptosis [11, 12]. Therefore, we next explored whether GSDME was expressed and cleaved to form GSDME-NT (37 kDa) in the drug-treated cells. The results showed that GSDME was cleaved by cisplatin in a time- and dose-dependent manner, which was correlated with the activation levels of caspase-3 (Fig. 4). Paclitaxel also time-dependently induced the cleavage of GSDME, but its efficiency was much weaker, consistent with the low levels of cleaved caspase-3 and -7, in comparison with cisplatin treatment (Fig. 4 and Supplementary Fig. 6). The cleavage of GSDME was also correlated with the levels of lytic cell death (Figs. 1, 2). These results indicated that cisplatin induced the activation of GSDME more robustly than paclitaxel did in A549 cells, suggesting that caspase-3-mediated cleavage of GSDME may have a role in determining the differential cell death induced by paclitaxel and cisplatin.

## Caspase-3-mediated cleavage of GSDME contributed to cisplatin-induced lytic cell death in A549 cells

As GSDME can only be cleaved by active caspase-3 to generate the GSDME-NT (37 kDa) fragment [11, 12], we subsequently investigated whether blockade of caspase-3 activation, by pre-treatment of the cells with its specific inhibitor Ac-DEVD-CHO (DEVD), attenuated the lytic cell death induced by paclitaxel or cisplatin. As expected, Western blotting showed that DEVD pre-treatment significantly suppressed the levels of cleaved GSDME (37 kDa) and cleaved PARP (89 kDa) in cisplatin-treated cells (Fig. 5a). However, paclitaxel-induced cleavage of GSDME was not suppressed by DEVD; the underlying mechanism is unclear. Consistent with these results, DEVD pre-treatment significantly inhibited cisplatin-, but not paclitaxel-, induced lytic cell death (PI-positive cells) (Fig. 5b, c, and Supplementary Fig. 7). These results indicated that caspase-3-mediated cleavage of GSDME contributed to cisplatin-induced lytic cell death and that the levels of GSDME-NT were correlated with the lytic cell death, suggesting that such lytic cell death is a form of secondary necrosis/pyroptosis.

## Expression of GSDME was a determinant of secondary necrosis/pyroptosis in A549 cells treated with paclitaxel and cisplatin

To further verify the role of GSDME in the secondary necrosis/pyroptosis induced by paclitaxel and cisplatin, we investigated whether GSDME knockdown by small interfering RNA (siRNA) could attenuate the secondary necrosis/pyroptosis in A549 cells. As shown in Fig. 6a, the expression of GSDME was reduced by ~90% after knockdown. PI staining showed that cisplatin-induced lytic cell death was also significantly reduced by GSDME knockdown as compared with control siRNA treatment (Fig. 6b, c, and Supplementary Fig. 8). The ratios of lytic cell death in paclitaxel groups were low and GSDME knockdown did not significantly reduced the lytic cell death. We also observed the morphology of dying cells using PI staining together with

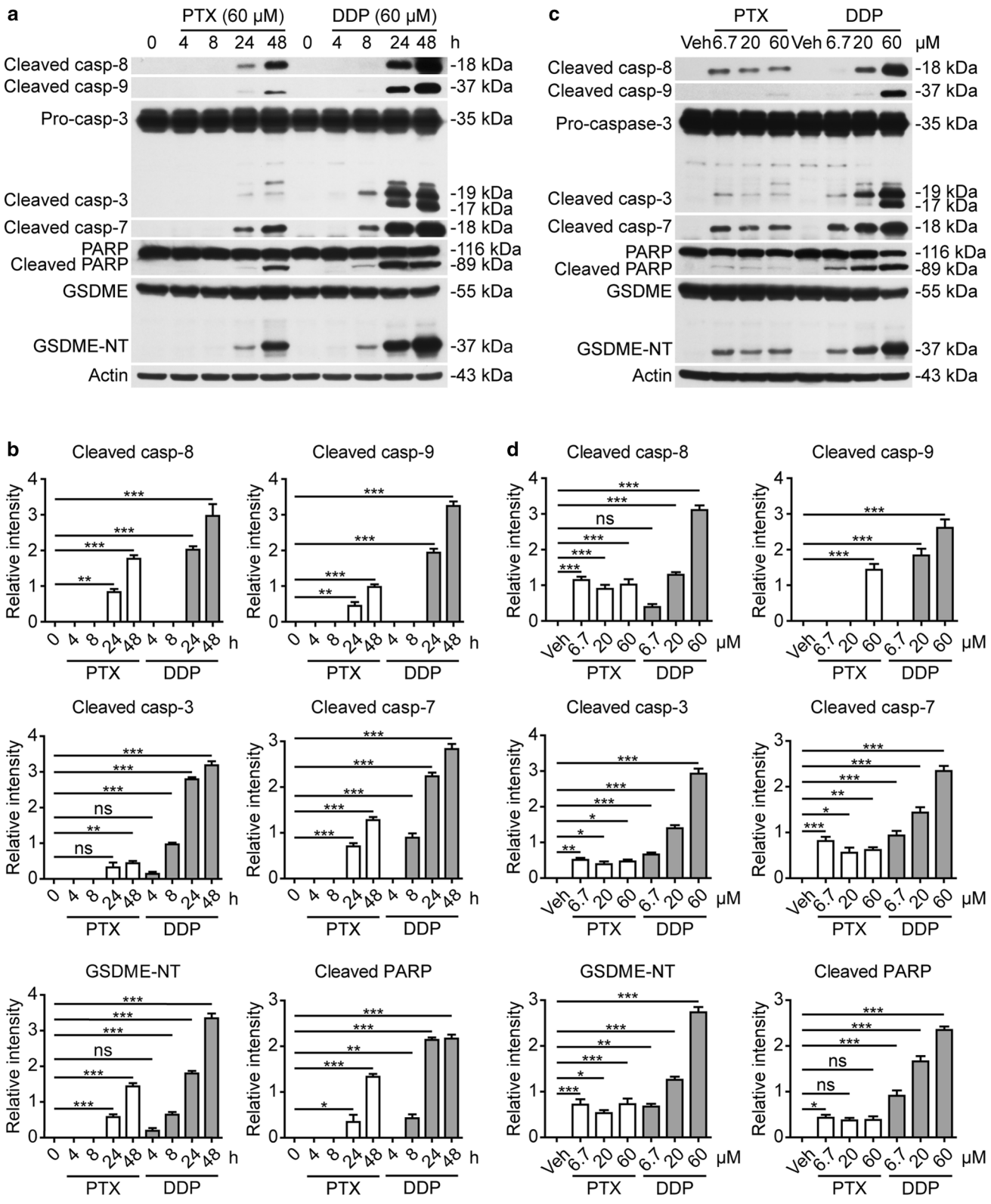


fluorescence microscopy. As shown in Fig. 6b, all the lytic dying cells (black arrow head) had large bubbles (yellow arrows) blowing from the plasma membrane after cisplatin treatment; GSDME knockdown reduced the number of cells with such features. Meanwhile, the cells with apoptotic morphology (PI-negative staining with cell shrinkage, white arrow head) in cisplatin-treated samples did not blow large bubbles with or without GSDME knockdown. Similar

◂**Fig. 4** Western blot analysis of apoptotic and lytic cell death markers in A549 cells treated with cisplatin or paclitaxel. **a, b** Cells were treated with 60 μM paclitaxel (PTX) or cisplatin (DDP) for 24 h. **a** After the cells were lysed by 2 × SDS–PAGE loading buffer, equal amounts of the total proteins in each sample were analyzed by Western blotting with indicated antibodies. Actin was recruited as a loading control. **b** Relative gray values of cleaved casp-8, cleaved casp-9, cleaved casp-3 (19 kDa), cleaved casp-7, cleaved PARP and GSDME-NT blots were quantified to respective actin blot. **c, d** Cells were treated with indicated concentrations of paclitaxel or cisplatin for 24 h, and then the cell lysates were assayed by Western blotting as in (**a**) followed by relative gray values analysis as in (**b**). Data are shown as mean ± SD ($n = 3$). $^{*}P < 0.05$; $^{**}P < 0.01$, $^{***}P < 0.001$; *ns* not significant, *Veh* vehicle

phenomena were observed in paclitaxel-treated cells, though only a small quantity of lytic dying cells each with a large bubble was induced by paclitaxel (60 μM, Supplementary Fig. 8). Besides, GSDME knockdown appeared to reduce the levels of apoptosis (PI-negative cells) in both paclitaxel- and cisplatin-treated cells (Fig. 6b). These results verified that GSDME was responsible, at least partly, for the lytic cell death (secondary necrosis/pyroptosis) induced by cisplatin.

Taken together, these results demonstrated that cisplatin was more potent than paclitaxel in inducing caspase-3/-7 activation and GSDME cleavage, and thus induced stronger secondary necrosis/pyroptosis in A549 cells that express GSDME protein.

## Discussion

Chemotherapy is one of the major strategies for cancer treatment, and paclitaxel and cisplatin are commonly-used chemotherapeutic agents [3, 4]. They are used for the treatment of many kinds of cancers including ovarian, cervical, breast and lung cancers. Mechanistically, both paclitaxel and cisplatin exhibit anticancer effects by inducing cell cycle arrest and apoptosis, which have been well-documented [14]. Consistent with previous findings, we in this study found that paclitaxel and cisplatin were able to induce typical signs of apoptosis in lung cancer A549 cells: detached from culture dish and rounding, positive for annexin-V staining, activation of apoptotic caspases (caspase-8, -9, -3 and -7) and cleavage of PARP. Interestingly, they also induced secondary necrosis/pyroptosis as judged by cell ballooning, the loss of membrane integrity and the participation of caspase-3 in the generation of GSDME-NT fragment (37 kDa) in this process. But cisplatin was much more potent in inducing such a cell death than paclitaxel. This study suggests that paclitaxel and cisplatin have differential effects on inducing inflammatory cell death in lung cancers expressing GSDME protein.

Recently, two forms of pyroptosis have been reported: one is mediated by cleaved GSDMD and the other is mediated by cleaved GSDME. The first form of pyroptosis is usually observed in immune cells upon inflammatory stimulations [such as lipopolysaccharide (LPS) priming plus ATP triggering, or LPS transfection into cells], which induce inflammasome and caspase-1/-4/-5/-11 activation. These caspases in turn cleave GSDMD to generate the N-terminal fragment (GSDMD-NT), which shapes pores in the plasma membrane [20–22]. The second form of pyroptosis has recently been reported by several studies, in which GSDME is cleaved by active caspase-3 to produce GSDME-NT that also has pore-forming activity in the plasma membrane, leading to pyroptosis in the chemotherapeutic agent-treated cancer cells as well as normal cells [11, 23]. This type of cell death caused by cleaved GSDME is also nominated as secondary necrosis, as it takes place downstream of chemotherapeutic agent-induced apoptosis [12, 14, 24]. As caspase-3 can execute both apoptosis and GSDME-mediated secondary necrosis/pyroptosis [11], one question is what determines the switch from apoptosis to secondary necrosis and another is whether all chemotherapeutic agents could induce secondary necrosis. For the first question, it is currently believed that the expression of GSDME is a determinant [11, 12]. Without GSDME expression, cells underdo apoptosis upon caspase-3 activation, whereas in cells expressing high level of GSDME protein, active caspase-3 further cleaves GSDME to generate GSDME-NT leading to secondary necrosis/pyroptosis. Consistent with previous studies [15], we found that cisplatin was more effective than paclitaxel both in generating GSDME-NT and in inducing lytic cell death in A549 cells. The generation of GSDME-NT was mediated by active caspase-3 as the caspase-3 specific inhibitor Ac-DEVD-CHO significantly inhibited GSDME cleavage and lytic cell death in cisplatin-treated cells. Furthermore, siRNA knockdown of *GSDME* expression significantly suppressed paclitaxel- and cisplatin-induced lytic cell death. Therefore, caspase-3-mediated GSDME cleavage was involved in the lytic cell death by paclitaxel and cisplatin in A549 cells, indicating that such lytic cell death was secondary necrosis/pyroptosis.

For the second question, our current study provides a line of evidence that different chemotherapeutic agents may induce different level of secondary necrosis/pyroptosis in a cell line with GSDME expression. Our study showed that in A549 cells expressing GSDME, cisplatin induced almost similar levels of apoptosis and secondary necrosis/pyroptosis whereas paclitaxel caused predominantly apoptosis with low levels of lytic cell death, consistent with the low levels of GSDME-NT upon paclitaxel treatment. The mechanism underlying this phenomenon is unclear. One possible explanation for this is that these two chemotherapeutic agents induced sharply different activation of caspases including caspase-8/-9/-3 at the same concentration and incubation time, thus producing different levels of GSDME-NT. Consistent with the finding that caspase-3 is the only caspase that cleaves GSDME [11], cisplatin-induced high levels of

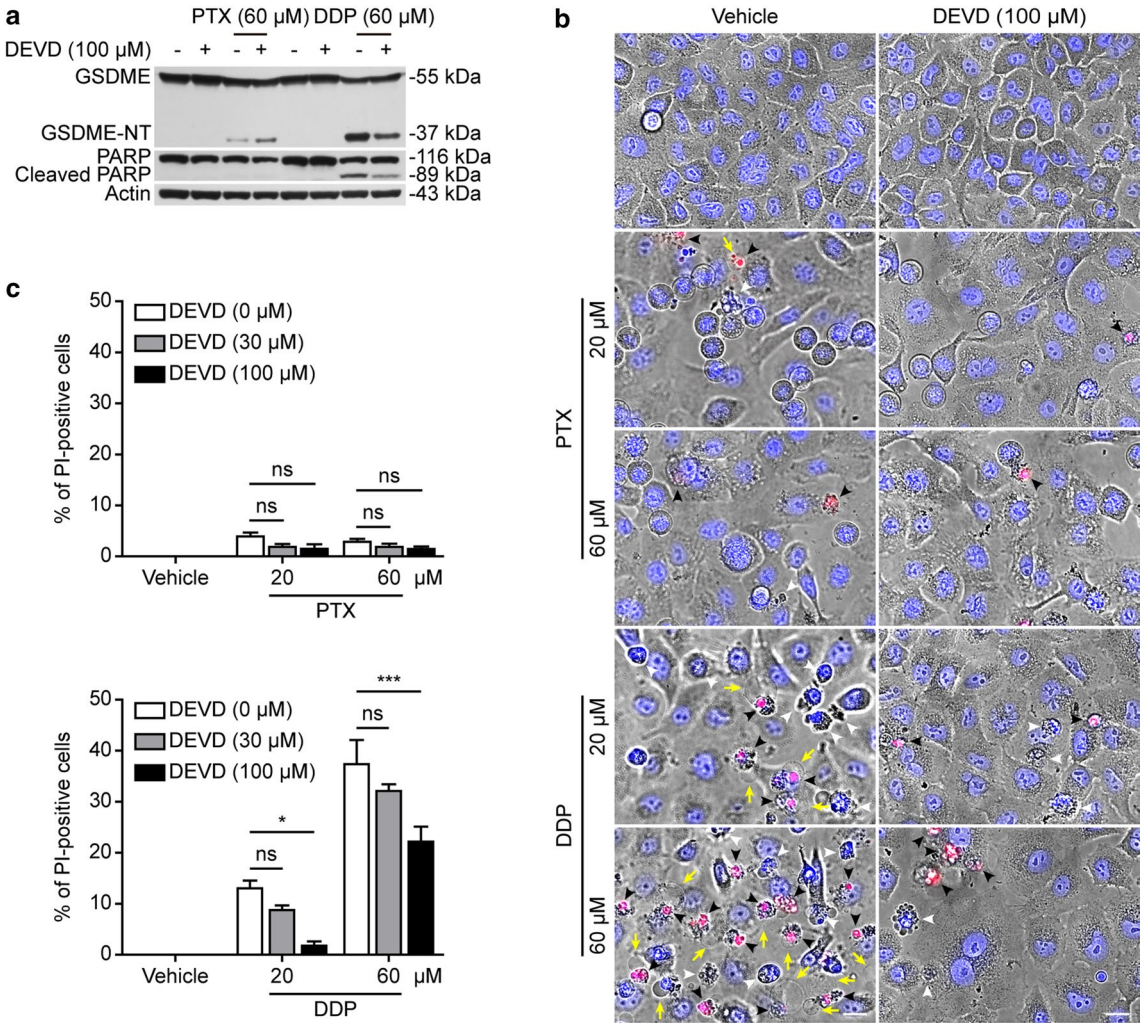


**Fig. 5** Blockade of caspase-3 activity suppressed cisplatin-induced lytic cell death. Cells were pre-treated with indicated concentrations of caspase-3 inhibitor Ac-DEVD-CHO (DEVD) for 1 h, and then treated with paclitaxel (PTX) or cisplatin (DDP), respectively, for 24 h. **a** Proteins in cell lysates were evaluated by Western blotting. Actin was used as a loading control. **b, c** Lytic cell death was assayed by propidium iodide (PI) and Hoechst 33342 staining. **b** A representative set of images (40×objective lens) of three independent experiments are shown. White arrow heads indicate apoptotic cells; black arrow heads indicate PI-positive (necrotic) cells; and yellow arrows indicate pyroptotic cells with large bubbles blowing form the cellular membrane. Scale bars, 20 μm. **c** PI-positive cells in five random fields (20×objective lens, around 100–150 cells per field) were calculated and statistically analyzed. Data are shown as mean ± SD ($n=5$). $^{*}P<0.05$; $^{***}P<0.001$; *ns* not significant

caspase-3 activation was correlated with robust cleavage of GSDME, while paclitaxel-induced low levels of caspase-3 was associated with low GSDME-NT levels (Fig. 4). Perhaps a certain amount of GSDME-NT was required to induce secondary necrosis but the low levels of GSDME-NT in paclitaxel-treated cells only induced a small number of cells with the typical phenotype of cell ballooning (i.e., large bubble). Despite of this, a number of typical pyroptotic cells with PI-positive staining and large bubbles were observed in high concentration- and 48 h-paclitaxel treated cells. Along this line, the upstream caspase-8 and -9 that activate caspase-3 were correspondingly activated in those cells treated with cisplatin or paclitaxel. This raises another question: why paclitaxel (60 μM) and cisplatin (60 μM) induced similar apoptosis but they caused different activation of caspase-8 and -9? One possibility is that they have different action mechanisms on lung cancer A549 cells: paclitaxel targeting microtubules could trigger mitochondrial apoptotic pathway as revealed by reduced mitochondrial membrane potential ($\Delta\Psi m$) in previous and this studies [25], whereas cisplatin acting as a DNA crosslinking agent may cause catastrophic damages to genomic DNA thus leading to robust activation of apoptosis initiator caspase-8/-9 [8–10]. In support of this, damage of genomic DNA has been reported to induce both intrinsic and extrinsic apoptotic pathways strongly, leading to the activation of the executioner capase-3 and -7 [10].

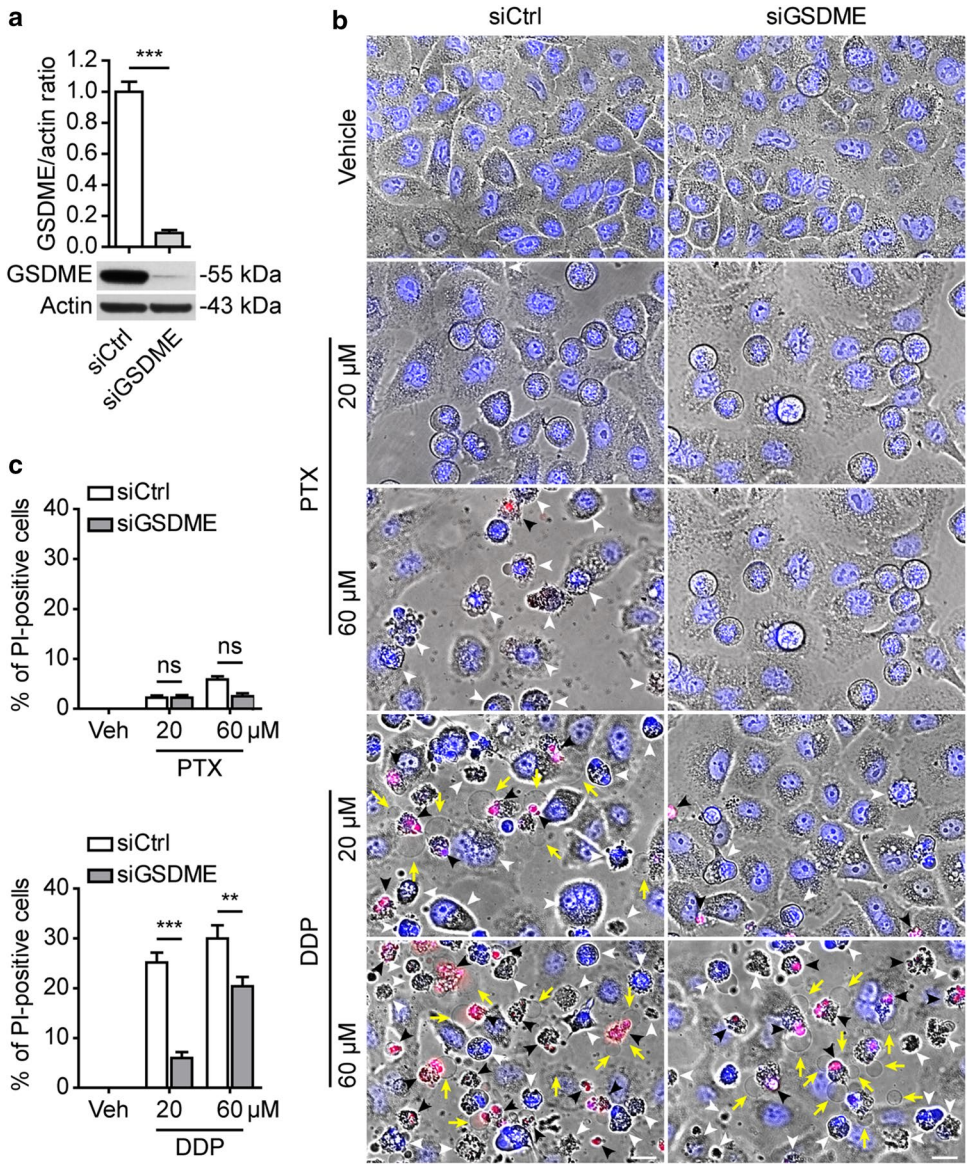


**Fig. 6** GSDME knockdown attenuated cisplatin-induced pyroptosis. **a** A549 cells were transfected with negative control siRNA (siCtrl) or GSDME siRNA (siGSDME) for 72 h. The knockdown efficiency of GSDME siRNA was analyzed by Western blotting and quantified by relative gray to actin. **b, c** After GSDME was knocked down as shown in (**a**), the cells were treated with graded concentrations of paclitaxel (PTX) or cisplatin (DDP) for 24 h. Lytic cell death were assayed by propidium iodide (PI) and Hoechst 33342 staining, and then the fluorescent images were captured by fluorescence microscopy. **b** One representative set of images (40 × objective lens) of three independent experiments are shown. White arrow heads indicate apoptotic cells; black arrow heads indicate PI-positive (necrotic) cells; and yellow arrows indicate pyroptotic cells with large bubbles blowing form the cellular membrane. Scale bars, 20 μm. **c** PI-positive cells in five random fields (around 100–150 cells per field, 20 × objective lens) were calculated and statistically analyzed. Data are shown as mean ± SD ($n = 5$). $^{**}P < 0.01$, $^{***}P < 0.001$; *ns* not significant, *Veh* vehicle

Two other DNA topoisomerase inhibitors, CPT-11 and etoposide, also induced secondary necrosis/pyroptosis in A549 cells and the latter seemed more effective in inducing such a phenomenon (Supplementary Figs. 3 and 4). Consistent with these observations, we found in this study that caspase-8, -9 and -3 were more potently activated by cisplatin as compared with paclitaxel treatment (Fig. 4 and Supplementary Fig. 6). Accordingly, the levels of cleaved GSDME and PARP (a substrate of caspase-3/-7) protein levels were much higher in cisplatin-treated cells as compared to paclitaxel-treated ones, considering that some of the cells treated with cisplatin had been lytic thus being lost during washing while only the proteins in the remaining cell lysates were evaluated in this study. On the other hand, paclitaxel has been shown to be a mimetic of lipopolysaccharide (LPS), a ligand of Toll-like receptor 4 (TLR4) that triggers the MyD88-NF-κB signaling [26]. Intriguingly, both TLR4 and MyD88 are expressed in A549 cells, and they have been reported to be associated with paclitaxel resistance in this cell line [19]. Paclitaxel resistance in A549 cells was also endorsed in this study, but the mechanism why GSDME-dependent necrosis was delayed in paclitaxel-treated A549 cells is still unclear. Therefore, whether induction of apoptosis by chemotherapeutic agents leads to secondary necrosis/pyroptosis or not is likely dependent on their action mechanisms, treatment time and levels of GSDME-NT generated in the cells. A schematic diagram illustrating the action of paclitaxel and cisplatin in inducing GSDME-mediated pyroptosis is shown in Fig. 7.

GSDME is a substrate of caspase-3, an executive enzyme in both apoptotic and pyroptotic pathways. However, the function of GSDME is largely unclear. Previous

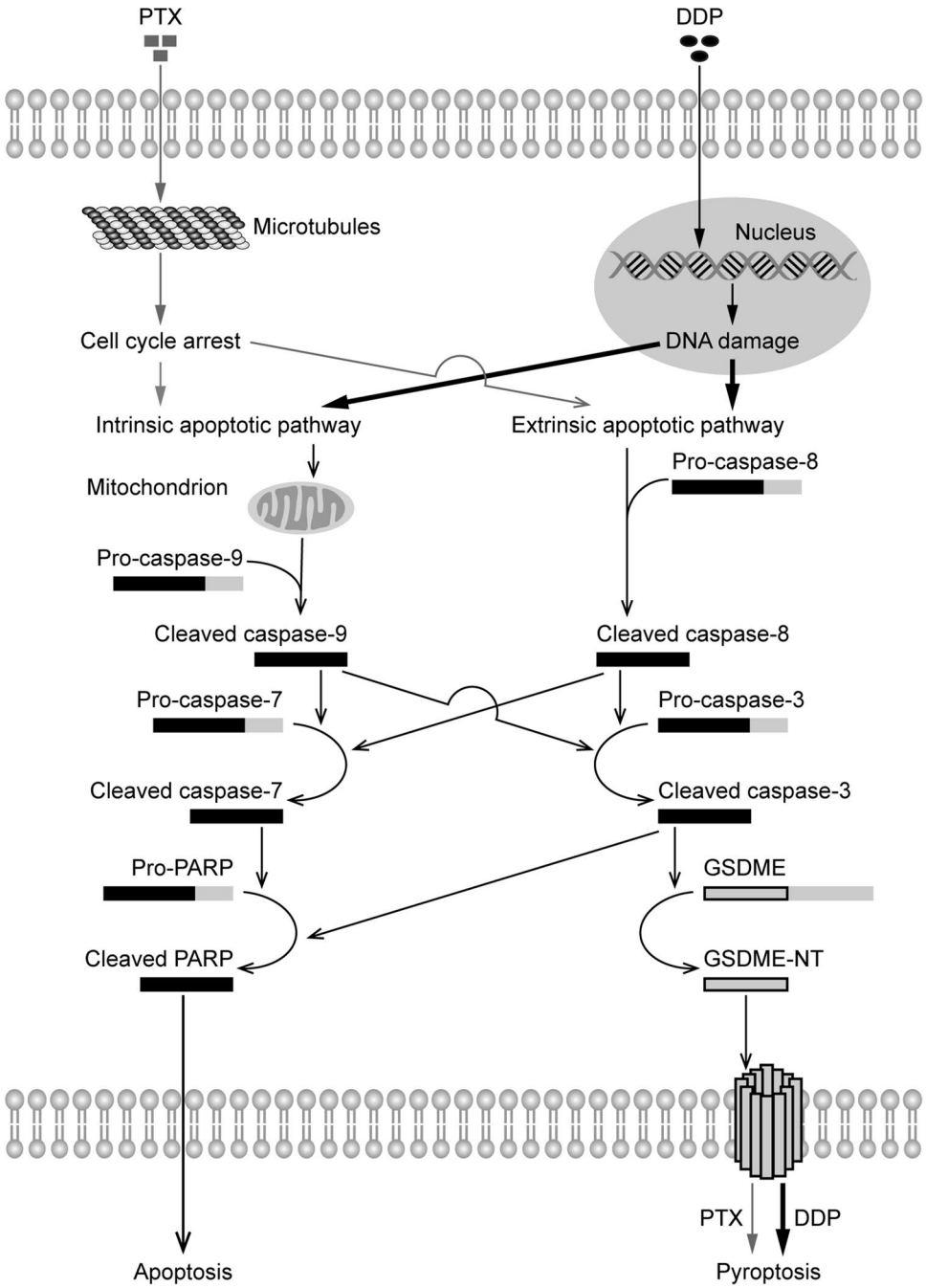


**Fig. 7** Schematic illustrating the induction of apoptosis and pyroptosis by paclitaxel and cisplatin. Paclitaxel targets microtubule and cisplatin targets genomic DNA. Both intrinsic and extrinsic apoptotic pathways were differentially activated by these drugs, resulting in different levels of GSDME cleavage and pyroptosis

findings has implicated its potential role in inducing apoptosis upon the treatment of DNA damage agents such as etoposide, through binding of tumor suppressor TP53 to the intron 1 of *GSDME* gene thus increasing GSDME expression [27]. Mutation in this gene leads to nonsyndromic hearing impairment (possibly due to deficiency of apoptosis in development) [28]. Its action in regulating pyroptosis has been revealed only recently [11, 12]. As a tumor suppressor gene, GSDME is not expressed in many cancers including gastric, colorectal and breast types [29]. However, It is constitutively expressed in A549 cells ([15] and Figs. 4, 5 of this study), suggesting that besides GSDME, other factors such as TP53 had contributed to the discrepancy of paclitaxel and cisplatin in inducing apoptosis and pyroptosis. Supporting these studies, we observed that *GSDME* knockdown not only reduced pyroptosis, but also decreased apoptosis (Fig. 6, indicated by black and white arrow heads, respectively) in both paclitaxel- and cisplatin-treated cells. It was likely that reduction of GSDME expression by siRNA diminished apoptosis, leading to decreased secondary necrosis/pyroptosis. But the exact mechanism warrants more investigation.

Although the *GSDME* gene is down-regulated or even silenced in many human cancer cells [30–32], it is expressed in lung cancer cells [11]. This means that lung cancers can be targeted to induce secondary necrosis/pyroptosis by chemotherapeutic drugs. Supporting this notion, recent studies have shown that molecular targeted therapies with protein kinase inhibitors were able to induce apoptosis concurrently with GSDME-dependent secondary necrosis/pyroptosis in lung cancer cells through the mitochondrial intrinsic apoptotic pathway, thus exhibiting anti-cancer effects *in vitro* and *in vivo* [15]. However, our study raises a concern that due to their distinct action mechanisms, chemotherapeutic agents may display different capability in inducing GSDME-mediated secondary necrosis/pyroptosis even in cells expressing high level of GSDME protein. Thus, cisplatin may provide additional advantages (including enhancement of immune responses) over paclitaxel by inducing secondary necrosis/pyroptosis in lung cancer cells expressing GSDME, which warrants further investigation. On the other hand, it has been reported that *GSDME*/*DFNA5* promoter was frequently methylated in primary breast cancers [30] and GSDME expression may be up-regulated by treatment of epigenetic drugs. Similarly, *GSDME*/*DFNA5* was down-regulated in gastric cancer cell lines due to methylation of its promoter region, and treatment with DNA methyltransferase inhibitor 5′-aza-2′-deoxycytidine (decitabine) restored GSDME/DFNA5 expression in these cells [15]. Thus, decitabine in combination with conventional chemotherapy drugs are more effective than each alone [33]. However, the efficacy of such a combination therapy may also be determined by what chemotherapeutic agent used, as GSDME expression is only a prerequisite for, but does not necessarily lead to, such secondary necrosis/pyroptosis. Together with our data presented in this study, decitabine combined with cisplatin may have advantages, in comparison to combination with paclitaxel, in treating cancers that have down-regulated *GSDME*/*DFNA5* expression, which warrants further research.

In contrast to cancer cells, GSDME is expressed in normal tissues including lung, kidney, spleen and intestinal epithelium, suggesting that induction of GSDME-mediated secondary necrosis/pyroptosis by chemotherapy can do harm to normal tissues [11]. In mice, cisplatin treatment results in intestinal and other tissue injuries leading to severe immune cell infiltration, but is less harmful to *Gsdme*$^{-/-}$ mice as compared to wild type mice [11]. This may partly explain the adverse toxicity of cisplatin in clinic [8]. To optimize their use in cancer treatment, their action mechanisms including induction of secondary necrosis/pyroptosis require more investigation.

In summary, our data demonstrated that both paclitaxel and cisplatin induced apoptosis and GSDME-mediated secondary necrosis/pyroptosis, but cisplatin triggered the secondary necrosis/pyroptosis more potently than paclitaxel did in A549 cells. This suggests that their potentials in triggering inflammatory responses and tissue damages were also different, which should be taken into consideration when using these drugs for cancer treatment. Our data may also provide a theoretical basis for the application of cisplatin in the treatment of cancers expressing GSDME protein.

**Acknowledgements** This work was supported by the grants from the National Natural Science Foundation of China (Nos. 81873064, 81773965 and 81673664).

## Compliance with ethical standards

**Conflict of interest** The authors declare no conflicts of interest.

## References

1. Chen W, Zheng R, Baade PD, Zhang S, Zeng H, Bray F, Jemal A, Yu XQ, He J (2016) Cancer statistics in China, 2015. CA Cancer J Clin 66(2):115–132. https://doi.org/10.3322/caac.21338
2. Siegel RL, Miller KD, Jemal A (2015) Cancer statistics, 2015. CA Cancer J Clin 65(1):5–29. https://doi.org/10.3322/caac.21254
3. Priyadarshini K, Keerthi AU (2012) Paclitaxel against cancer: a short review. Med Chem 2(7):139–141. https://doi.org/10.4172/2161-0444.1000130
4. Fennell DA, Summers Y, Cadranel J, Benepal T, Christoph DC, Lal R, Das M, Maxwell F, Visseren-Grul C, Ferry D (2016) Cisplatin in the modern era: the backbone of first-line chemotherapy for non-small cell lung cancer. Cancer Treat Rev 44:42–50. https://doi.org/10.1016/j.ctrv.2016.01.003
5. Arnal I, Wade RH (1995) How does taxol stabilize microtubules? Curr Biol 5(8):900–908. https://doi.org/10.1016/S0960-9822(95)00180-1
6. Piperno G, LeDizet M, Chang XJ (1987) Microtubules containing acetylated alpha-tubulin in mammalian cells in culture. J Cell Biol 104(2):289–302. https://doi.org/10.1083/jcb.104.2.289
7. Ganguly A, Yang H, Cabral F (2013) Detection and quantification of microtubule detachment from centrosomes and spindle poles. Methods Cell Biol 115(20):49–62. https://doi.org/10.1016/B978-0-12-407757-7.00004-9
8. Florea AM, Busselberg D (2011) Cisplatin as an anti-tumor drug: cellular mechanisms of activity, drug resistance and induced side effects. Cancers 3(1):1351–1371. https://doi.org/10.3390/cancers3011351
9. Dasari S, Tchounwou PB (2014) Cisplatin in cancer therapy: molecular mechanisms of action. Eur J Pharmacol 740:364–378. https://doi.org/10.1016/j.ejphar.2014.07.025
10. Roos WP, Kaina B (2006) DNA damage-induced cell death by apoptosis. Trends Mol Med 12(9):440–450. https://doi.org/10.1016/j.molmed.2006.07.007
11. Wang YP, Gao WQ, Shi XY, Ding JJ, Liu W, He HB, Wang K, Shao F (2017) Chemotherapy drugs induce pyroptosis through caspase-3 cleavage of a gasdermin. Nature 547(7661):99–103. https://doi.org/10.1038/nature22393
12. Rogers C, Fernandes-Alnemri T, Mayes L, Alnemri D, Cingolani G, Alnemri ES (2017) Cleavage of DFNA5 by caspase-3 during apoptosis mediates progression to secondary necrotic/pyroptotic cell death. Nat Commun 8:14128. https://doi.org/10.1038/ncomms14128

13. Coleman ML, Sahai EA, Yeo M, Bosch M, Dewar A, Olson MF (2001) Membrane blebbing during apoptosis results from caspase-mediated activation of ROCK I. Nat Cell Biol 3(4):339–345. https://doi.org/10.1038/35070009
14. Hassan M, Watari H, AbuAlmaaty A, Ohba Y, Sakuragi N (2014) Apoptosis and molecular targeting therapy in cancer. Biomed Res Int 2014:150845. https://doi.org/10.1155/2014/150845
15. Lu H, Zhang S, Wu J, Chen M, Cai MC, Fu Y, Li W, Wang J, Zhao X, Yu Z, Ma P, Zhuang G (2018) Molecular targeted therapies elicit concurrent apoptotic and GSDME-dependent pyroptotic tumor cell death. Clin Cancer Res. https://doi.org/10.1158/1078-0432.CCR-18-1478
16. Jian W, Bai Y, Li X, Kang J, Lei Y, Xue Y (2018) Phosphatidylethanolamine-binding protein 4 promotes the epithelial-to-mesenchymal transition in non-small cell lung cancer cells by activating the sonic hedgehog signaling pathway. J Cell Biochem https://doi.org/10.1002/jcb.27817
17. Py BF, Jin M, Desai BN, Penumaka A, Zhu H, Kober M, Dietrich A, Lipinski MM, Henry T, Clapham DE, Yuan J (2014) Caspase-11 controls interleukin-1beta release through degradation of TRPC1. Cell Rep 6(6):1122–1128. https://doi.org/10.1016/j.celrep.2014.02.015
18. Zha QB, Wei HX, Li CG, Liang YD, Xu LH, Bai WJ, Pan H, He XH, Ouyang DY (2016) ATP-induced inflammasome activation and pyroptosis is regulated by AMP-activated protein kinase in macrophages. Front Immunol 7:597. https://doi.org/10.3389/fimmu.2016.00597
19. Xiang F, Wu R, Ni Z, Pan C, Zhan Y, Xu J, Meng X, Kang X (2014) MyD88 expression is associated with paclitaxel resistance in lung cancer A549 cells. Oncol Rep 32(5):1837–1844. https://doi.org/10.3892/or.2014.3433
20. Shi J, Zhao Y, Wang K, Shi X, Wang Y, Huang H, Zhuang Y, Cai T, Wang F, Shao F (2015) Cleavage of GSDMD by inflammatory caspases determines pyroptotic cell death. Nature 526(7575):660–665. https://doi.org/10.1038/nature15514
21. Baker PJ, Boucher D, Bierschenk D, Tebartz C, Whitney PG, D'Silva DB, Tanzer MC, Monteleone M, Robertson AA, Cooper MA, Alvarez-Diaz S, Herold MJ, Bedoui S, Schroder K, Masters SL (2015) NLRP3 inflammasome activation downstream of cytoplasmic LPS recognition by both caspase-4 and caspase-5. Eur J Immunol 45(10):2918–2926. https://doi.org/10.1002/eji.201545655
22. Kayagaki N, Stowe IB, Lee BL, O'Rourke K, Anderson K, Warming S, Cuellar T, Haley B, Roose-Girma M, Phung QT, Liu PS, Lill JR, Li H, Wu J, Kummerfeld S, Zhang J, Lee WP, Snipas SJ, Salvesen GS, Morris LX, Fitzgerald L, Zhang Y, Bertram EM, Goodnow CC, Dixit VM (2015) Caspase-11 cleaves gasdermin D for non-canonical inflammasome signalling. Nature 526(7575):666–671. https://doi.org/10.1038/nature15541
23. Wang Y, Yin B, Li D, Wang G, Han X, Sun X (2018) GSDME mediates caspase-3-dependent pyroptosis in gastric cancer. Biochem Biophys Res Commun 495(1):1418–1425. https://doi.org/10.1016/j.bbrc.2017.11.156
24. Kaufmann SH, Earnshaw WC (2000) Induction of apoptosis by cancer chemotherapy. Exp Cell Res 256(1):42–49. https://doi.org/10.1006/excr.2000.4838
25. Ly JD, Grubb DR, Lawen A (2003) The mitochondrial membrane potential ($\Delta\psi m$) in apoptosis; an update. Apoptosis 8(2):115–128. https://doi.org/10.1023/A:1022945107762
26. Byrd-Leifer CA, Block EF, Takeda K, Akira S, Ding A (2001) The role of MyD88 and TLR4 in the LPS-mimetic activity of taxol. Eur J Immunol 31(8):2448–2457. https://doi.org/10.1002/1521-4141(200108)31:8<2448::aid-immu2448>3.0.co;2-n
27. Masuda Y, Futamura M, Kamino H, Nakamura Y, Kitamura N, Ohnishi S, Miyamoto Y, Ichikawa H, Ohta T, Ohki M, Kiyono T, Egami H, Baba H, Arakawa H (2006) The potential role of DFNA5, a hearing impairment gene, in p53-mediated cellular response to DNA damage. J Hum Genet 51(8):652–664. https://doi.org/10.1007/s10038-006-0004-6
28. Van Laer L, Huizing EH, Verstreken M, van Zuijlen D, Wauters JG, Bossuyt PJ, Van de Heyning P, McGuirt WT, Smith RJ, Willems PJ, Legan PK, Richardson GP, Van Camp G (1998) Nonsyndromic hearing impairment is associated with a mutation in DFNA5. Nat Genet 20(2):194–197. https://doi.org/10.1038/2503
29. de Beeck KO, Van Laer L, Van Camp G (2012) DFNA5, a gene involved in hearing loss and cancer: a review. Ann Otol Rhinol Laryngol 121(3):197–207. https://doi.org/10.1177/000348941212100310
30. Kim MS, Lebron C, Nagpal JK, Chae YK, Chang X, Huang Y, Chuang T, Yamashita K, Trink B, Ratovitski EA, Califano JA, Sidransky D (2008) Methylation of the DFNA5 increases risk of lymph node metastasis in human breast cancer. Biochem Biophys Res Commun 370(1):38–43. https://doi.org/10.1016/j.bbrc.2008.03.026
31. Akino K, Toyota M, Suzuki H, Imai T, Maruyama R, Kusano M, Nishikawa N, Watanabe Y, Sasaki Y, Abe T, Yamamoto E, Tarasawa I, Sonoda T, Mori M, Imai K, Shinomura Y, Tokino T (2007) Identification of DFNA5 as a target of epigenetic inactivation in gastric cancer. Cancer Sci 98(1):88–95. https://doi.org/10.1111/j.1349-7006.2006.00351.x
32. Kim MS, Chang X, Yamashita K, Nagpal JK, Baek JH, Wu G, Trink B, Ratovitski EA, Mori M, Sidransky D (2008) Aberrant promoter methylation and tumor suppressive activity of the DFNA5 gene in colorectal carcinoma. Oncogene 27(25):3624–3634. https://doi.org/10.1038/sj.onc.1211021
33. Ball B, Zeidan A, Gore SD, Prebet T (2017) Hypomethylating agent combination strategies in myelodysplastic syndromes: hopes and shortcomings. Leuk Lymphoma 58(5):1022–1036. https://doi.org/10.1080/10428194.2016.1228927